

See discussions, stats, and author profiles for this publication at: <https://www.researchgate.net/publication/51564667>

Tribological Properties of Self-Assembled Monolayers of Catecholic Imidazolium and the Spin-Coated Films of Ionic Liquids

ARTICLE *in* LANGMUIR · AUGUST 2011

Impact Factor: 4.46 · DOI: 10.1021/la201378b · Source: PubMed

CITATIONS

11

READS

57

9 AUTHORS, INCLUDING:



Jianxi Liu

Karlsruhe Institute of Technology

25 PUBLICATIONS 279 CITATIONS

SEE PROFILE



Bo Yu

Chinese Academy of Sciences

63 PUBLICATIONS 1,230 CITATIONS

SEE PROFILE



Feng Zhou

Chinese Academy of Sciences

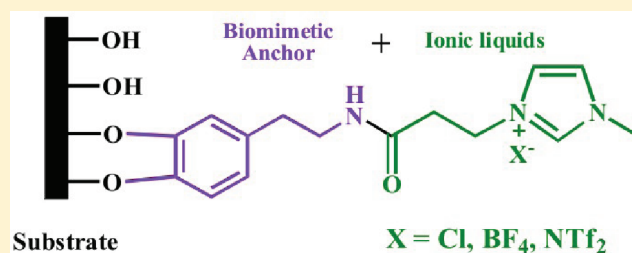
257 PUBLICATIONS 6,320 CITATIONS

SEE PROFILE

Tribological Properties of Self-Assembled Monolayers of Catecholic Imidazolium and the Spin-Coated Films of Ionic Liquids

Jianxi Liu,^{†,‡} Jinlong Li,[†] Bo Yu,^{*,†} Baodong Ma,[§] Yangwen Zhu,[§] Xinwang Song,[§] Xulong Cao,[§] Wu Yang,[‡] and Feng Zhou^{*,†}[†]State Key Laboratory of Solid Lubrication, Lanzhou Institute of Chemical Physics, Chinese Academy of Sciences, Lanzhou 730000, PR China[‡]College of Chemistry and Chemical Engineering, Northwest Normal University, Lanzhou 730070, PR China[§]Geology Institute, Shengli Oilfield, Dongying 257015, PR China

ABSTRACT: A novel compound of an imidazolium type of ionic liquid (IL) containing a biomimetic catecholic functional group normally seen in mussel adhesive proteins was synthesized. The IL can be immobilized on a silicon surface and a variety of other engineering material surfaces via the catecholic anchor, allowing the tribological protection of these substrates for engineering applications. The surface wetting and adhesive properties and the tribological property of the synthesized self-assembled monolayers (SAMs) are successfully modulated by altering the counteranions. The chemical composition and wettability of the IL SAMs were characterized by means of X-ray photoelectron spectroscopy (XPS) and contact angle (CA) measurements. The adhesive and friction forces were measured with an atomic force microscope (AFM) on the nanometer scale. IL composite films were prepared by spin coating thin IL films on top of the SAMs. The macrotribological properties of these IL composite films were investigated with a pin-on-disk tribometer. The results indicate that the presence of IL SAMs on a surface can improve the wettability of spin-coated ionic liquids and thus the film quality and the tribological properties. These films registered a reduced friction coefficient and a significantly enhanced durability and load-carrying capacity. The tribological properties of the composite films are better than those of pure IL films because the presence of the monolayers improves the adhesion and compatibility of spin-coated IL films with substrates.



1. INTRODUCTION

Micro/nanoelectrical mechanical systems (M/NEMS) provide great potential for applications in areas such as mechatronics and medical and sensor technologies.^{1,2} A large surface area-to-volume ratio in miniaturized devices causes serious adhesive and frictional problems for their operation.^{3,4} These devices cannot be lubricated with conventional liquid lubricants or even physically deposited films because of their normally large thickness. Therefore, lubrication with molecular films such as self-assembled monolayers (SAMs) is a promising choice in resolving tribological problems owing to their close-packed structures and strong bonding to the substrates and thus their thermodynamic stability.^{3,5–8} Three SAM systems are most commonly used: thiols on noble metals,^{9,10} silanes on silicon-based materials,¹¹ and phosph(on)ates on metal oxides.¹² In general, a limitation has been that the binding chemistry to be applied is determined by the surface chemistry of the substrate materials.¹³ Recently, it was reported that catechol-based (Dopamine) adhesive compounds can bond strongly to a wide variety of substrates at high binding strength, including metals (Ag, Au),^{14,15} native oxide surfaces (Ti, Cu, and Fe),^{16–18} semiconductors (Si),¹⁹ and polymers.²⁰ For example, Rodenstein et al.²¹ have reported the fabrication of chemical gradients on oxide surfaces by catechol-based SAMs. The catechol-based anchoring chemistry

emerges as a very promising biomimetic approach to surface functionalization.

Ionic liquids (ILs) have been used in many applications, including uses as nonvolatile solvents,²² electrolytes,²³ and chromatographic stationary phases²⁴ because of their unique characteristics such as negligible volatility, nonflammability, high thermal stability, low melting point, and conductivity. Compared with normally used synthetic oils, ILs, which are promising alternatives, have shown remarkable lubrication and antiwear properties^{25–29} due to the fact that the characteristics of ILs are just what high-performance lubricants demand and the high polarity of ILs makes them able to form very strong effective adsorption films and gives them the ability to participate in tribochemical reactions.^{30,31} Imidazolium-based ILs have been widely studied as base oils, additives, and thin films because of their excellent stability, flexibility in molecular design, ease of synthesis, and adaptability to multiple functions. The potential of ILs in thin film lubrication has been exploited by a number of researchers and by our group.^{32–36} Lee et al.³⁷ have reported the formation of imidazolium ion-terminated SAMs on Au having

Received: May 25, 2011

Revised: July 19, 2011

Published: August 11, 2011

different anions and the effects of counteranions on surface hydrophilicity and hydrophobicity. Because the catecholic IL SAMs possess imidazolium terminal groups and can be strongly bonded on a variety of substrate surfaces, they show excellent microtribological performance and possess good adhesion-resistant ability. However, SAMs exhibit unfavorable antiwear durability.^{38–40} Compared with SAMs, fluid lubrication possesses long-term endurance, the promotion of thermal conductance, and a high load-carrying capacity but usually has to face the problematic issue of dewetting.³¹ Therefore, to improve the tribological behavior of thin film lubrication further and to acquire insight into their potential in resolving the tribological problems of MEMS, composite films containing chemically bonded SAMs and spin-coated thin films on top can be expected for significantly better tribological properties such as a better friction-reducing, antiwear ability and a much better load-carrying capacity.

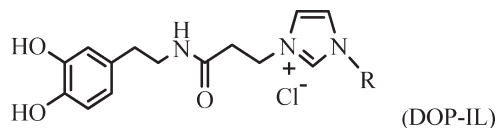
In the present work, we combine ionic liquids with catecholic attachment chemistry and have synthesized a novel catecholic imidazolium molecule. It was then immobilized onto a silicon substrate, and the surface properties of the IL SAMs and the tribological behavior exhibited by exchanging the counteranions was studied. Beyond that, the tribological properties of spin-coated thin IL films above DOP-IL SAMs were studied. Considering the wide substrate adaptability of catecholic attachment chemistry, this technique provides a simple and effective method of delivering IL monolayers on a variety of substrates of interest for engineering lubrication applications.

2. EXPERIMENTAL SECTION

Materials. Single-crystal silicon (100) wafers were purchased from GRINM Semiconductor Materials Co. Ltd. (Beijing, China). 3-Hydroxytyramine hydrochloride (dopamine·HCl) and lithium bis-(trifluoromethanesulphonyl)imide (LiNTf₂) were obtained from Aldrich. 1-Ethyl-3-(3-dimethylaminopropyl) carbodiimide hydrochloride (EDC·HCl) and *N*-hydroxysuccinimide (NHS) were purchased from Shanghai Fine Chemical Co. Ltd. (Shanghai, China). 1-Hexyl-3-methylimidazolium tetrafluoroborate (L-B106) used to spin coat films in this study was synthesized according to ref 22. All other chemicals used in this work were analytical grade and used as received. Deionized water was used throughout the experiments.

Synthesis of 1-*N*-[2-(3,4-Dihydroxyphenyl)ethyl]propionamide-3-methylimidazolium Chloride (DOP-IL). The structure of DOP-IL is shown in the following text, and the synthesis procedures are briefly described here. 3-Chloropropionic acid (0.23 g, 2.10 mmol), EDC·HCl (0.40 g, 2.10 mmol), and NHS (0.10 g, 0.42 mmol) were dissolved in 15 mL of deionized water in an ice–water bath, and the solution was stirred under N₂ for 15 min (solution A). Solution B was prepared by dissolving Na₂CO₃ (0.11 g, 1.26 mmol) in 20 mL of deionized water, the solution was stirred under N₂ for 15 min, and dopamine·HCl (0.48 g, 2.52 mmol) was added with another 15 min of degassing. Then, solution B was added to solution A and stirred for another 30 min in an ice–water bath and for 12 h at 35 °C thereafter. Then the reaction mixture was acidified to pH 2 with 1 M HCl (aqueous) and extracted with EtOAc (3 × 50 mL). The combined organic extracts were dried over anhydrous MgSO₄, and the solvent was evaporated under reduced pressure to give a light-brown liquid. The crude product was purified by silica gel column chromatography (4% MeOH in CHCl₃) to give a colorless viscous liquid (0.16 g, 0.66 mmol, yield 31.5%). The product (0.51 g, 2.1 mmol) and 1-methylimidazole (0.17 g, 2.1 mmol) were added to a 250 mL round-bottomed flask containing 20 mL of isopropanol under N₂ protection and stirred for 48 h at 75 °C.

Then the solvent was removed on a rotary evaporator, and the residue was placed on a silica gel chromatography column and eluted with 10% MeOH in CHCl₃.



Preparation of Self-Assembled Monolayers. Silicon wafers were cleaned and hydroxylated by exposure to O₂ plasma (Femto, diener electronic) for 3 min (at a power of 99 W). The wafers were then immersed in a 1 mM acetone solution of DOP-IL for 24 h for surface immobilization. After modification, the wafers were rinsed with water and dried in a stream of N₂. For the fabrication of DOP-IL monolayers with different counteranions, the modified substrates were placed in 0.1 M NaBF₄ and LiNTf₂ solutions for 10 min of anion exchange.

Preparation of IL Composite Films. A solution of 0.5% (w/v) L-B106 IL in acetone was prepared for spin coating. A 15 μ L drop of the L-B106 solution was spin coated onto the substrates having DOP-IL SAMs (with different counteranions: Cl, BF₄, and NTf₂) at 3600 rpm for 60 s with a 4W-4A spin coater (Beijing, China). Then the IL composite film samples were heat treated at 100 °C for 3 h. The samples were named L-B106, L-B106-Cl, L-B106-BF₄, and L-B106-NTf₂, respectively. L-B106 and DOP-IL having Cl counteranions were spin coated onto the bare silicon substrate under the same conditions and were named L-B106 and DOP, respectively.

Characterization of the Films. The chemical composition of the DOP-IL monolayers was measured by X-ray photoelectron spectroscopy (XPS), which was carried out on a PHI-5702 multifunctional spectrometer using Al K α radiation. The binding energies were referenced to the C 1s line at 284.6 eV from adventitious carbon. The static water contact angles of DOP-IL SAMs were measured by the sessile drop method in a DSA100 (Kruss) telescopic goniometer. A 5 μ L droplet of deionized water was used in the measurements with five replicate measurements for each specimen. A dynamic contact angle measurement system (DCAT11, DataPhysics, Germany) was reconfigured and used to test the adhesive force between a droplet of water and sample surfaces by recording force–displacement curves. In this work, a 5 μ L water droplet is used for the force measurement.

AFM measurements were performed using a Multimode AFM (Nanoscope IIIa, Veeco Instrument, Santa Barbara, CA). To measure adhesive and friction forces, standard commercially available, 100- μ m-long, wide-legged, V-shaped Si₃N₄ cantilevers with a nominal spring constant of 0.58 N/m (NP-10, Digital Instruments) were used. The spring constant for individual silicon nitride cantilevers was calculated from the measurements of their resonance frequencies using the microscope software and was based on the method reported by Hutter and Bechhoefer.⁴¹ Adhesive forces between the AFM tip and specimen were determined from typical force–distance curves. Herein, we used the force–volume (FV) mapping technique to obtain the adhesive force per unit area and the statistical distribution.⁴² The friction force was measured under a constant load using a 90° scan angle. The scan length was 1 μ m, and the scan frequency was 1 Hz.

The macrotribological behaviors of the IL composite films were examined on a UMT-2MT tribometer (CETR Corporation Ltd., USA) in a ball-on-disk configuration. The counterpart was a GCr15 steel ball (\varnothing 3 mm, SAES2100) that was cleaned ultrasonically, before experiments, in acetone and ethanol for 10 min. All tests were conducted under ambient laboratory conditions. The worn surfaces of the films were observed on a MicroXAM 3D noncontact profilometer (ADE Phase Shift Inc., USA) in phase mode.

3. RESULTS AND DISCUSSION

Formation and Characterization of Monolayers. It is well known that catechol derivatives can form stable complexes with silicon.¹⁹ Figure 1 shows the structure of the catecholic imidazolium molecule immobilized on a Si–OH surface.

To confirm the successful covalent attachment of DOP-IL molecules onto silicon surface, XPS survey spectra analysis (Figure 2) was used to analyze the presence of anions associated with the imidazole ring for surface functionalization. In all spectra of DOP-IL SAMs, the N 1s signals centered at 400.4 eV indicate the successful covalent attachment of DOP-ILs on the silicon surface. For the SAMs of DOP-Cl, the Cl 2p signal appears at 198.6 eV (Figure 2b). The signals of F 1s and B 1s appear at 685.8 and 192.4 eV for DOP-BF₄ SAMs (Figure 2c), and those of F 1s and S 2p appear at 685.4 and 166.6 eV for DOP-NTf₂ (Figure 2d), respectively. A plausible mechanism for the adsorption of DOP-IL on the Si surface is suggested by Frye,⁴³ who verified the reaction of catechol with organic silica to yield organosilicon salts. Messersmith and co-workers¹⁶ reported the depletion of surface Ti–OH groups after modification with

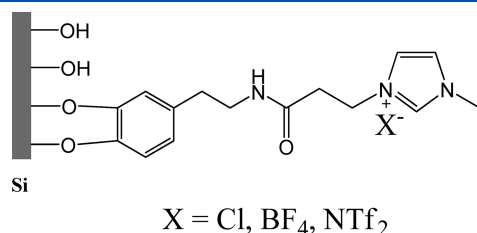


Figure 1. Self-assembled monolayers of DOP-ILs immobilized on a silicon substrate.

DOPA catechol polymers, suggesting a similar binding mechanism. Thus, a dehydration reaction between catechol and the Si–OH surface might occur, leading to a chemical bond between catecholic molecules and the substrate surface and the formation of imidazolium-molecule-terminated monolayers.

Wettability and Adhesion. The surface hydrophilicity and hydrophobicity of the IL SAMs can be easily tuned by presenting imidazolium ions at the tail ends having different anions.³⁷ The utilization of the tunable properties of the ILs in surface science could provide a new way to control the properties of the surfaces. As an example, fluorinated ILs are hydrophobic with low hygroscopicity and can be used as lubricants.⁴⁴ In this work, the wettability of the DOP-IL SAMs having different anions (Cl, BF₄, and NTf₂) was investigated. The corresponding water contact angles are shown in Figure 3, and the images of water droplets on sample surfaces were inserted into the figure. The contact angle of the silicon substrate was 0°, and it was changed to 35° after DOP-Cl SAMs were assembled on the substrate. The contact angles became greater through the exchange of the counteranions with BF₄ (51°) and NTf₂ (74°). The results indicate that the wettability of the DOP-IL SAMs surface could be tailored by changing the anions. The nature of the anion has a greater influence on the surface wettability of DOP-IL SAMs, with wettability decreasing in the order of Cl > BF₄ > NTf₂. When imidazolium is coupled with a chlorine anion, the ion pair can dissociate and the terminus has a high water affinity and is hydrophilic. SAMs coupled with NTf₂ anions are known to be the most hydrophobic counteranions among the three and have the lowest hydration capability, so the surface shows the highest water contact angle. The anion effect on the surface wettability demonstrated herein is of general significance to the adsorption on molecular surfaces. This effect could be advantageously incorporated into the design of monolayer-based technologies

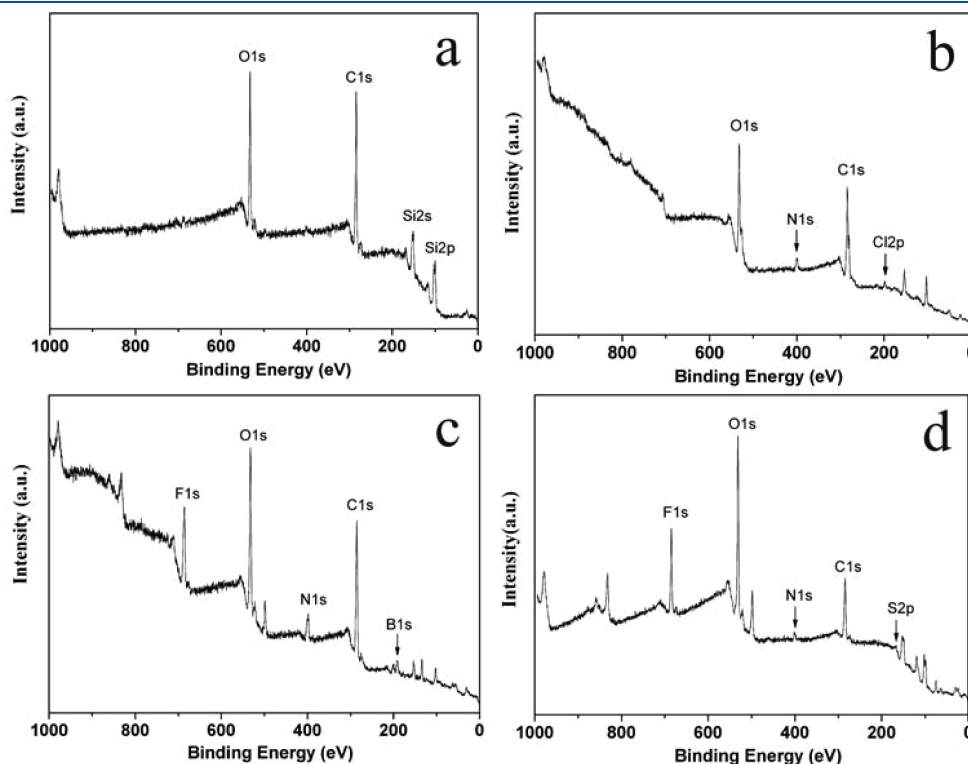


Figure 2. XPS survey spectra of (a) a silicon substrate and surfaces modified with (b) DOP-Cl, (c) DOP-BF₄, and (d) DOP-NTf₂.

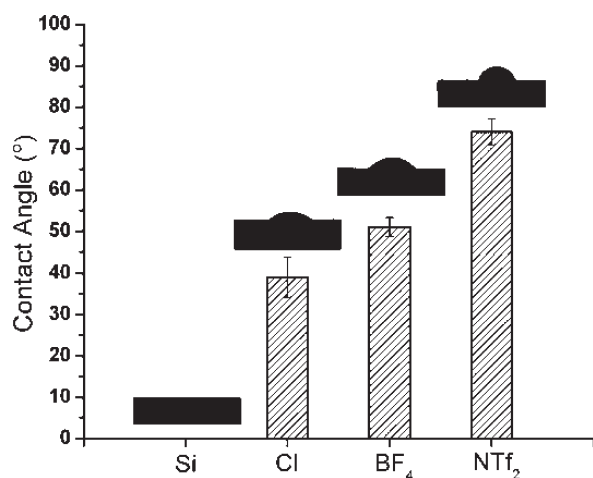


Figure 3. Water contact angles of the silicon wafers modified with DOP-IL SAMs.

such as microfluidics and microdevices used in anion sensing and in biomedical areas.

The adhesive force between a water droplet and a solid surface is an effective way to characterize the surface wettability because surfaces with different contact angles have different adhesive forces. In our work, when the dynamic contact angle measurement system started to work, the sample approached the water droplet, made contact, and then moved back, and the whole process of sample stage movement versus force change was recorded by instrument-matched software. The adhesive force was defined as the force required to take the water droplet away from the sample surface and can be measured by using a high-sensitivity microelectronic balance system.⁴⁵

Figure 4 shows the force–displacement curve by water droplet measured on DOP-IL-modified silicon surfaces. As is known, the silicon surface is hydrophilic, it exhibits remarkable adhesion to water droplets, and has the highest adhesive force of approximately 618 μN . The adhesive force of the DOP-Cl-modified silicon surface decreases to 480 μN . By exchanging the counteranions with BF₄ and NTf₂, the adhesive force decreased gradually from 408 and 354 μN , which implies a further reduction in surface wettability. This result has a good correlation with the water contact angle measurement.

AFM offers a facile way to characterize the microscopic physicochemical and mechanical properties of SAMs. A force–distance curve contains information about the nanoscale interaction force between the AFM tip and the surface, which is related to changes in the surface energy. To study the adhesive force statistically, a force–volume test was employed to extend the adhesive force measurement from a point to the entire surface. The tip scans across the sample surface within a $1\ \mu\text{m} \times 1\ \mu\text{m}$ surface area, and an adhesive force map of 64×64 resolution can be obtained synchronously with topographical image. Therefore, the changes in surface adhesion are displayed on the map intuitively and analyzed by histograms.

Figure 5 shows the FV (left column) and respective adhesion histograms (right column) of the surface adhesion force distribution calculated from these images. The adhesive forces were acquired between a silicon nitride tip and the DOP-IL SAMs with different counteranions. It can be seen that a relatively homogeneous adhesive forces are shown over the entire $1\ \mu\text{m} \times 1\ \mu\text{m}$ surface area of all of the DOP-IL SAMs, which indicates that

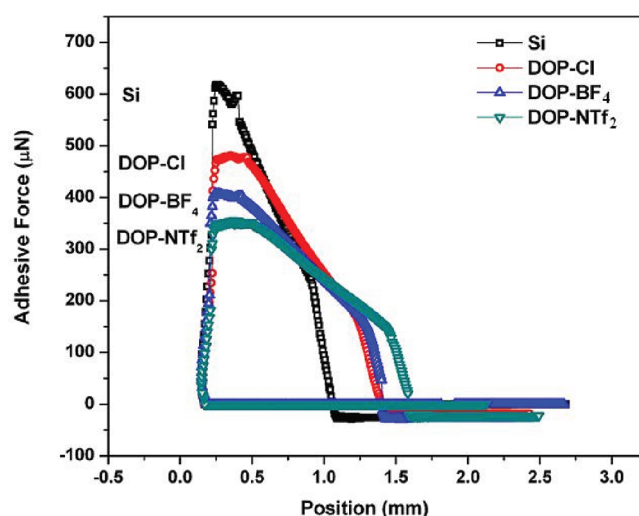


Figure 4. Force–displacement curve measured between DOP-IL SAM-modified silicon surfaces and a water droplet.

densely packed DOP-IL SAMs exists on silicon substrates. The calculated mean adhesive force value of the Si substrate is $45.7 \pm 1.4\ \text{nN}$. After DOP-IL has been assembled on the Si surface, the adhesion force decreases to $43.4 \pm 1.6\ \text{nN}$ for DOP-Cl SAMs. As the counteranions of the SAMs are exchanged for BF₄ and NTf₂, the adhesive forces decrease to 38.6 ± 2.1 and $37.7 \pm 3.1\ \text{nN}$, respectively.

Tsukruk⁴⁶ summarized that the surface properties of SAMs depend on the variation of the surface energy of solids, which is mainly determined from the functional terminations, orientation, and conformation. In our present work, the surface energy of DOP-IL SAMs was modulated only by exchanging the small counteranions (Cl) with BF₄ and NTf₂, so the adhesive force of the SAMs was decreased along with the reduction in surface energy.

We can conclude that the variation of the adhesive force of the IL-modified Si surfaces is a quantitative illustration of the successful exchange of the counteranions of DOP-IL SAMs on the Si surface. Strong adhesion is observed on the Si surface, which is wholly covered with hydroxyl groups and is hydrophilic. The hydrophilicity decreased after DOP-Cl was assembled on the Si substrate and decreased more when the counteranions of DOP-ILs were exchanged with BF₄ and NTf₂. This indicates that IL SAMs with BF₄ and NTf₂ counteranions have good adhesion resistance because the fluorinated counteranions are hydrophobic. Such a phenomenon is well understood because the adhesion dominated by the capillary force between the tip and the surface is dramatically lowered or even eliminated when the surface becomes hydrophobic. The results are well correlated with the contact angle measurements.

To measure the friction force of DOP-IL SAMs, a lateral force microscope (LFM) was used to study the friction force in an air environment. Because the lateral spring constant of the V-shaped cantilever and the lateral sensitivity of the optical detector were not measured, the collected friction signals here were voltages, and a relative friction force was obtained, which is to be in proportion to the absolute friction force. The applied normal load was controlled by transforming the set point voltage. At least five separate locations from which to collect the friction signals under variable applied loads for each sample were selected.

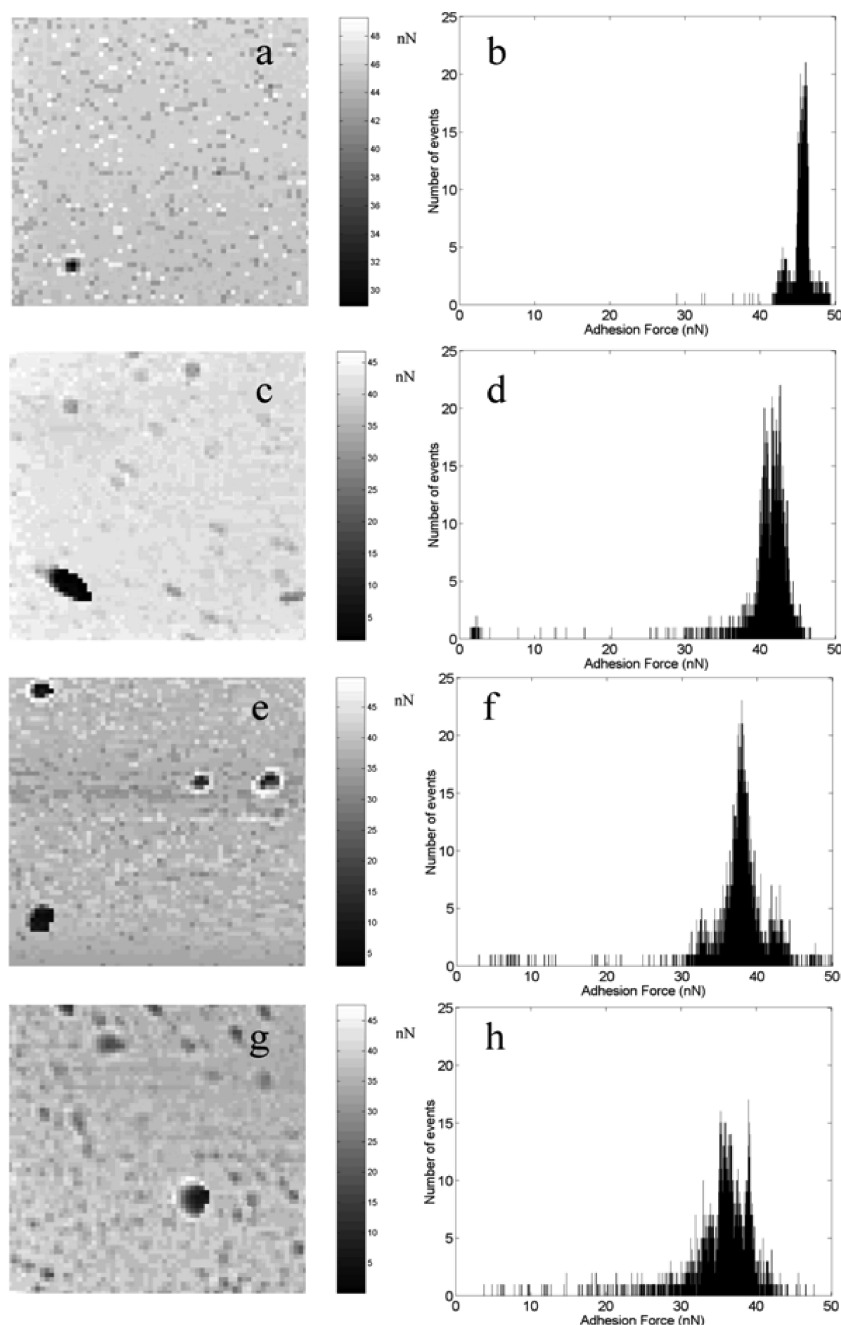


Figure 5. Force–volume adhesion images (left column) of the Si substrate and DOP-IL SAMs and the corresponding adhesion histograms (right column): (a, b) silicon substrate and surfaces modified with (c, d) DOP-Cl, (e, f) DOP-BF₄, and (g, h) DOP-NTf₂.

Figure 6 shows the variation in friction force data versus the applied load for the Si and modified Si substrates. To analyze the data, a linear fit was made over the entire force range based on the modified Amonton's law:^{47,48} $F_L = \mu F_N + F_0$ where μ , F_N , and F_0 are the coefficient of friction, applied normal load, and adhesive-force-related friction force (at a zero normal load). The adhesion between the AFM tip and the sample surface makes a considerable contribution to interfacial friction. It can be seen that a good linear relationship between the friction force and the normal load is acquired for DOP-IL SAMs with different counteranions. Si substrates possess a highest friction force of $3.77F_N + 249.34$. The friction force decreased to $3.38F_N + 195.74$ after the DOP-Cl IL

was assembled on the substrate to form a protective film, followed by counteranion exchanges (BF₄ and NTf₂), which are $2.85F_N + 199.47$ and $2.69F_N + 139.96$, respectively. It can be observed that all of the DOP-IL SAMs reduce the friction force.

A molecular spring model raised by Bhushan et al.⁴⁹ suggests that because the SAMs have compliant features and can experience orientation and be compressed under a normal load, the tip is likely to slide on top of a molecular spring when the AFM tip slides on the SAM surface. The compliant features reduce the shearing force at the interface, so the friction is reduced. A large nonzero friction signal is observed at zero normal load for the hydroxylated silicon surface, which is attributed to the jump-to-contact

instability caused by attractive forces during the approach of the tip to the sample surface.

Srinivasan et al.⁵⁰ reported that $\text{CF}_3(\text{CF}_2)_7(\text{CH}_2)_2\text{SiCl}_3$ (FDTS) SAMs cause the surface energy of SiO_2 to decrease by 4 orders of magnitude, and the antiadhesion and friction properties were improved significantly when the SiO_2 surface was modified by FDTS. In our work, the surface energy decreased after the anions of DOP-IL SAMs were exchanged with fluoro-containing anions (BF_4^- and NTf_2^-), and NTf_2^- is larger than BF_4^- ,

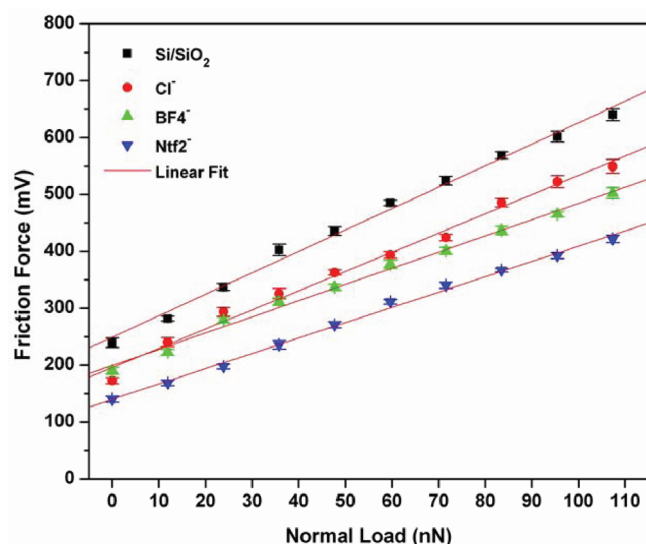


Figure 6. Friction force data vs applied load for the Si substrate and DOP-IL SAMs. The solid lines are linear regression lines.

even more than Cl^- . This reflects that the silicon surface has a large surface energy.⁵¹ On the basis of the observed friction force of the DOP-ILs, it could be possible to quantify the effects of counteranions on the tribological behavior of assembled imidazolium-based ILs, which follows the trend of $\text{Cl}^- > \text{BF}_4^- > \text{NTf}_2^-$. This indicates that the low friction of the DOP-IL SAMs could be attributed to the lower surface energy, especially for the NTf_2^- counteranion where the adhesive-force-related friction force is the lowest, comparatively. Such behavior is also consistent with the adhesive results (Figure 5).

Macrotribological Behavior Characterization. Synthetic ionic liquids used as lubricants exhibit excellent tribological behavior, which is reported by many researchers. Meanwhile, the catecholic IL SAMs possessing imidazolium terminal groups exhibit excellent microtribological performance and possess the good adhesion-resistant ability mentioned above. In this section, we try to investigate the macrotribological properties of DOP-IL SAMs on silicon. To improve the wear-resistance properties of DOP-IL SAMs, composite IL films were applied to investigate the tribological properties. The macrotribological properties of the films were tested on a UMT-2MT tribometer. The sliding frequency and the length were kept constant at 3 Hz and 5 mm, respectively, and the applied loads are 0.2, 0.5, and 1.0 N. The period of time that the friction test was carried out was 30 min, except for wear out (an abrupt rise in the friction coefficient).

Figure 7a shows the variation in the friction coefficient relative to time for the spin-coated films where the applied normal load is 0.2 N. It can be seen that the average friction coefficient for all of the films remains stable over 1800 s. The IL composite film of L-B106- NTf_2^- is stable, and the lowest friction coefficient is about 0.06. The average friction coefficients of the L-B106- Cl^- and L-B106- BF_4^- films are a little higher than that of the L-B106- NTf_2^-

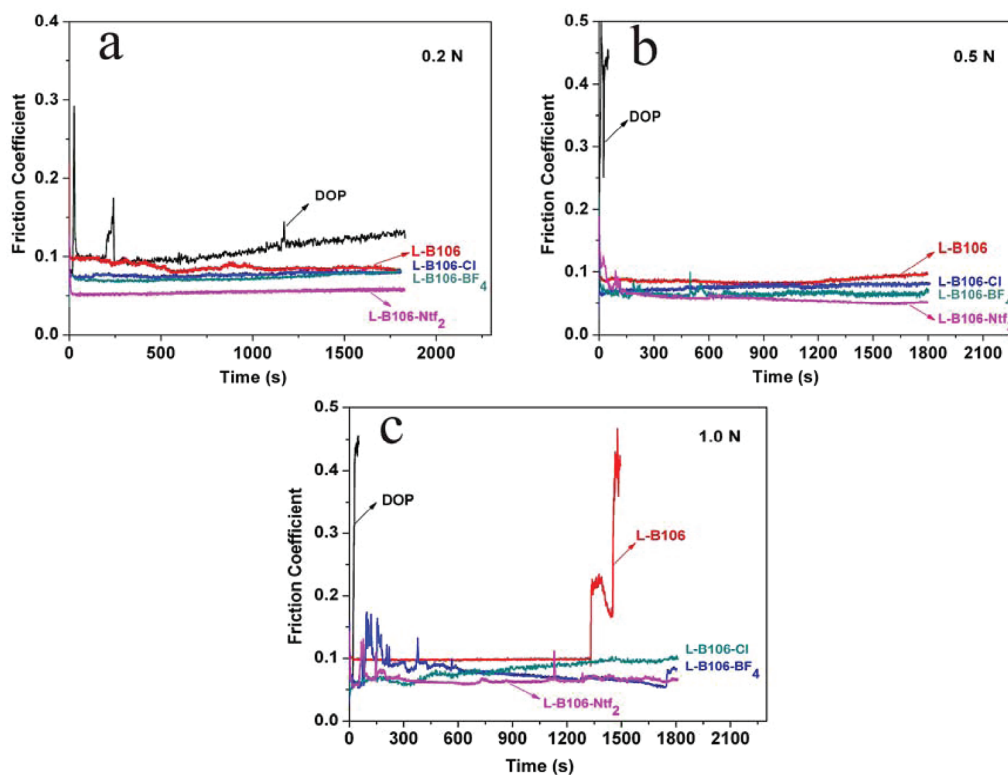


Figure 7. Variation in friction coefficient with time for the IL composite films. The films were tested under applied normal loads of 0.2, 0.5, and 1.0 N, sliding against a GCr15 steel ball ($\varnothing 3$ mm, SAE52100). The sliding frequency and the length were kept constant at 3 Hz and 5 mm.

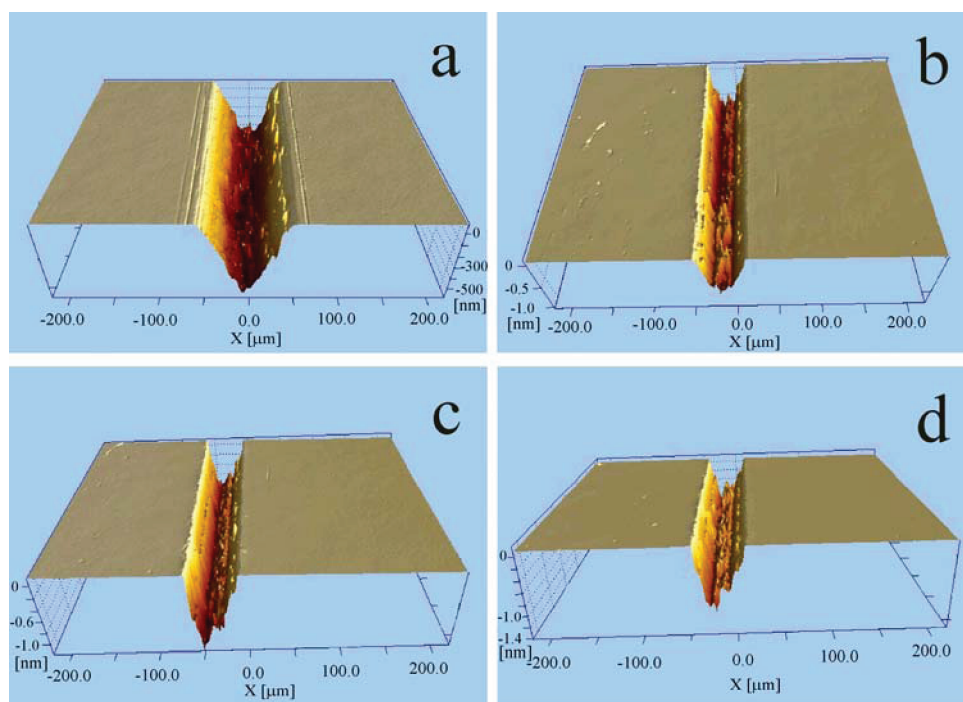


Figure 8. Three-dimensional noncontact profilometer images of the worn surfaces of the IL composite films under a load of 1.0 N: (a) L-B106, (b) L-B106-Cl, (c) L-B106-BF₄, and (d) L-B106-NTf₂.

film and remain at the same level of about 0.08. Comparatively, the initial friction coefficient for the pure L-B106 film is about 0.1 but fluctuates; however, it finally returns to about 0.08. The friction coefficient of the DOP film increases gradually from 0.09 to 0.13 over 1800 s.

Figure 7b shows the friction coefficient for the IL composite films at an applied load of 0.5 N. The DOP film was worn out in 5 s and shows little wear resistance, and the friction coefficient is about 0.40. This may contribute to the fact that DOP-Cl is solid and has low fluidity at ordinary temperatures. The L-B106 film reveals comparatively better tribological properties than the DOP film under an applied normal load of 0.5 N, where a friction coefficient of 1.0 is observed. The composite films have much better wear resistance and relatively lower friction coefficients of about 0.08 and 0.07 for L-B106-Cl and L-B106-BF₄, respectively. The average friction coefficient for the L-B106-NTf₂ film remains the lowest at 0.06.

As the applied load increased to 1.0 N (Figure 7c), the DOP film could not bear the higher loads and was worn out in the initial state. The average friction coefficient of a spin-coated film of L-B106 remains stable at about 0.1 until 1330 s (when it abruptly increased to about 0.22) and then abruptly increases to 0.4 at about 1400 s, where it was apparent that the film failed. On the contrary, the composite films remained steady at 0.1 and 0.08 for the L-B106-Cl and L-B106-BF₄ films. The friction coefficient of the L-B106-NTf₂ film was quite stable at about 0.07.

From the above information, we can find that the composite films have the ability to withstand load, especially L-B106-NTf₂, which possesses the lowest friction coefficient. L-B106-Cl and L-B106-BF₄ films also have a comparatively good load-carrying capacity. For the L-B106 film, the friction coefficient remains stable under low loads but the antiwear life is much shorter than that of composite films. The results have good

consistency with the corresponding mechanical study by AFM measurements.

To provide further information on the effectiveness of the IL composite films in reducing wear, a comparison of the wear properties of the silicon substrate spin-coated with pure L-B106 IL and DOP-IL SAMs modified with L-B106 films was conducted. The morphologies of the worn surface of the L-B106 and IL composite films under a load of 1.0 N were observed on a 3D noncontact profilometer as shown in Figure 8. It can be seen that the wear scar on the spin-coated L-B106 film is the deepest and widest when compared to those of the IL composite films of L-B106-Cl, L-B106-BF₄, and L-B106-NTf₂. That is to say that the wear resistance behavior of the IL composite films is better than that of pure spin-coated ILs and that the IL composite films have commendable wear resistance that is crucial to their potential application as a lubricant layer. We did not take an image of the spin-coated DOP film because it was worn out in the initial stage.

As a result, IL composite films have a sufficiently high mechanical strength to bear loads and a good wear-resistance ability. The enhanced wear resistance and load-carrying ability of the IL composite films should rely on a combination of SAMs and fluid film lubrication. The rigid, well-packed DOP-IL SAMs underlayer enhanced the stability and load-carrying capacity of the entire film, and it also enhanced the compatibility between the liquid and the underlying surface. The compatibility plays a key role in forming an effective thin film,⁵² which has a significant impact on the tribological properties of the IL composite films. Because L-B106 is water-insoluble, it has a poor film-formation ability on hydroxylated silicon surfaces. On the contrary, the ionic liquid could easily adsorb onto the DOP-IL SAMs to form an effective continuous film, which significantly decreases the friction and wear. Therefore, the IL composite films have good tribological properties.

4. CONCLUSIONS

We have synthesized a novel imidazolium type of IL containing a biomimetic catecholic anchor. The catecholic IL can be successfully immobilized on a silicon surface through a catecholic anchor, allowing the tribological protection of these substrates for engineering applications. The wettability, adhesion, and friction force for the catecholic IL SAMs were modulated by exchanging the counteranions, which all follow the trend of $\text{Cl}^- > \text{BF}_4^- > \text{NTf}_2^-$. Namely, the SAMs coupled with the NTf_2^- anion, the most hydrophobic counteranion among the testing anions, showed the highest water contact angle value and the lowest friction and adhesive forces. DOP-IL SAMs have good tribological properties under low load, and the catecholic IL SAMs, which bind to a variety of substrate surfaces, might be developed as a potential boundary lubricating layer. In addition, the IL spin-coated films of normal ILs on DOP-IL SAMs maintain a better load-carrying capacity and antiwear ability than do pure, normal IL films on substrates. It is hypothesized that the presence of IL SAMs on surfaces can improve the wettability of the film and thus the film quality and tribological properties. Thus, IL composite films might find promising applications in the lubrication of microelectromechanical systems (MEMS).

AUTHOR INFORMATION

Corresponding Author

*E-mail: yubo@licp.cas.cn; zhouf@licp.cas.cn. Tel: 86-931-4968466. Fax: 86-931-4968163.

ACKNOWLEDGMENT

This work was supported by the Hundred Talents Program of CAS and State key research project 2008ZX05011-002. We thank Dr. Jing Zhao for the force–volume analysis.

REFERENCES

- (1) Spearing, S. M. *Acta Mater.* **2000**, *48*, 179.
- (2) Bhushan, B.; Fuchs, H. *Applied Scanning Probe Methods*; Springer-Verlag: Heidelberg, Germany, 2006.
- (3) Bhushan, B.; Kulkarni, A. V.; Boehm, M.; Koinkar, V. N.; Odoni, L.; Martelet, C.; Belin, M. *Langmuir* **1995**, *11*, 3189.
- (4) Rymuza, Z. *Microsyst. Technol.* **1999**, *5*, 173.
- (5) Maboudian, R.; Howe, R. T. *J. Vac. Sci. Technol., B* **1997**, *15*, 1.
- (6) Liu, H.; Ahmed, I. U.; Scherge, M. *Thin Solid Films* **2001**, *381*, 135.
- (7) Clear, S. C.; Nealey, P. F. *Langmuir* **2001**, *17*, 720.
- (8) Ashurst, R.; Carraro, C. W.; Maboudian, R.; Frey, W. *Sens. Actuators, A* **2003**, *104*, 213.
- (9) Nuzzo, R. G.; Zegarski, B. R.; Dubois, L. H. *J. Am. Chem. Soc.* **1987**, *109*, 733.
- (10) Troughton, E. B.; Bain, C. D.; Whitesides, G. M.; Nuzzo, R. G.; Allara, D. L.; Porter, M. D. *Langmuir* **1988**, *4*, 365.
- (11) Chaudhury, M. K.; Whitesides, G. M. *Science* **1992**, *255*, 1230.
- (12) Tosatti, S. G. P.; Michel, R.; Textor, M.; Spencer, N. D. *Langmuir* **2002**, *18*, 3537.
- (13) Love, J. C.; Estroff, L. A.; Kriebel, J. K.; Nuzzo, R. G.; Whitesides, G. M. *Chem. Rev.* **2005**, *105*, 1103.
- (14) Kawabata, T. *Biochem. Pharmacol.* **1996**, *51*, 1569.
- (15) Brooksby, P. A.; Schiel, D. R.; Abell, A. D. *Langmuir* **2008**, *24*, 9074.
- (16) Dalsin, J. L.; Lin, L.; Tosatti, S. G. P.; Voros, J.; Textor, M.; Messersmith, P. B. *Langmuir* **2005**, *21*, 640.
- (17) Araujo, P. Z.; Morando, P. J.; Blesa, M. A. *Langmuir* **2005**, *21*, 3470.
- (18) Creutz, C.; Chou, M. H. *Inorg. Chem.* **2008**, *47*, 3509.
- (19) Lambert, J.; Singer, S. *J. Organomet. Chem.* **2004**, *689*, 2293.
- (20) Lee, H.; Dellatore, S. M.; Miller, W. M.; Messersmith, P. B. *Science* **2007**, *318*, 426.
- (21) Rodenstein, M.; Zürcher, S.; Tosatti, S. G. P.; Spencer, N. D. *Langmuir* **2010**, *21*, 16211.
- (22) Bonhote, P.; Dias, A. P.; Papageorgiou, N.; Kalyanasundaram, K.; Gratzel, M. *Inorg. Chem.* **1996**, *35*, 1168.
- (23) Li, J. H.; Shen, Y. F.; Zhang, Y. J.; Liu, Y. *Chem. Commun.* **2005**, 360.
- (24) Anderson, J. L.; Armstrong, D. W.; Wei, G.-T. *Anal. Chem.* **2006**, *78*, 2892.
- (25) Ye, C. F.; Liu, W. M.; Chen, Y. X.; Yu, L. G. *Chem. Commun.* **2001**, *21*, 2244.
- (26) Ye, C. F.; Liu, W. M.; Chen, Y. X.; Ou, Z. W. *Wear* **2002**, *253*, 579.
- (27) Liu, W. M.; Ye, C. F.; Gong, Q. Y.; Wang, H. Z.; Wang, P. *Tribol. Lett.* **2002**, *13*, 81.
- (28) Mu, Z. G.; Zhou, F.; Zhang, S. X.; Liang, Y. M.; Liu, W. M. *Tribol. Int.* **2005**, *38*, 725.
- (29) Liu, X. Q.; Zhou, F.; Liang, Y. M.; Liu, W. M. *Wear* **2006**, *261*, 1174.
- (30) Plechkova, N. V.; Seddon, K. R. *Chem. Soc. Rev.* **2008**, *37*, 123.
- (31) Zhou, F.; Liang, Y. M.; Liu, W. M. *Chem. Soc. Rev.* **2009**, *38*, 2590.
- (32) Yu, B.; Zhou, F.; Mu, Z.; Liang, Y. M.; Liu, W. M. *Tribol. Int.* **2006**, *39*, 879.
- (33) Yu, G.; Zhou, F.; Liu, W. M.; Liang, Y. M.; Yan, S. *Wear* **2006**, *260*, 1076.
- (34) Zhu, M.; Yan, J.; Mo, Y. F.; Bai, M. W. *Tribol. Lett.* **2008**, *29*, 177.
- (35) Palacio, M.; Bhushan, B. *Adv. Mater.* **2008**, *20*, 1194.
- (36) Bhushan, B.; Palacio, M.; Kinzig, B. J. *Colloid Interface Sci.* **2008**, *317*, 275.
- (37) Lee, B. S.; Chi, Y. S.; Lee, J. K.; Choi, I. S.; Song, C. E.; Namgoong, S. K.; Lee, S.-g. *J. Am. Chem. Soc.* **2004**, *126*, 480.
- (38) Ruehe, J.; Novotny, V. J.; Kanazawa, K. K.; Clarke, T.; Street, G. B. *Langmuir* **1993**, *9*, 2383.
- (39) Rye, R. R.; Nelson, G. C.; Dugger, M. T. *Langmuir* **1997**, *13*, 2965.
- (40) Patton, S. T.; William, D. C.; Eapen, K. C.; Zabinski, J. S. *Tribol. Lett.* **2000**, *9*, 199.
- (41) Hutter, J. L.; Bechhoefer, J. *Rev. Sci. Instrum.* **1993**, *64*, 1868.
- (42) Smith, D. A.; Connell, S. D.; Robinson, C.; Kirkham, J. *Anal. Chim. Acta* **2003**, *479*, 39.
- (43) Frye, C. L. *J. Am. Chem. Soc.* **1964**, *86*, 3170.
- (44) Phillips, B. S.; John, G.; Zabinski, J. S. *Tribol. Lett.* **2007**, *26*, 85.
- (45) Liu, J. X.; Yu, B.; Ma, B. D.; Song, X. W.; Cao, X. L.; Li, Z. Q.; Yang, W.; Zhou, F. *Colloids Surf., A* **2010**, *380*, 175.
- (46) Tsukruk, V. V. *Adv. Mater.* **2001**, *13*, 95.
- (47) Lee, D. H.; Oh, T.; Cho, K. J. *Phys. Chem. B* **2005**, *109*, 11301.
- (48) Ruths, M.; Granick, S. *J. Phys. Chem. B* **1998**, *102*, 6056.
- (49) Bhushan, B.; Liu, H. W. *Phys. Rev. B* **2001**, *63*, 245412.
- (50) Srinivasan, U.; Houston, M. R.; Howe, R. T.; Maboudian, R. *J. Microelectromech. Syst.* **1998**, *7*, 252.
- (51) Ren, S. L.; Yang, S. R.; Wang, J. Q.; Liu, W. M.; Zhao, Y. P. *Chem. Mater.* **2004**, *16*, 428.
- (52) Eapen, K.; Patton, S.; Smallwood, S.; Phillips, B.; Zabinski, J. *J. Microelectromech. Syst.* **2005**, *14*, 954.